Light nuclei production in a multiphase transport model for relativistic heavy ion collisions

Kai-Jia Sun[*] and Che Ming Ko[†]
Cyclotron Institute and Department of Physics and Astronomy, Texas A&M University, College Station, Texas 77843, USA

Zi-Wei Lin[‡]
Department of Physics, East Carolina University, Greenville, North Carolina 27858, USA

(Received 4 July 2020; revised 13 May 2021; accepted 1 June 2021; published 17 June 2021)

Based on an improved multiphase transport (AMPT) model, which gives a good description of proton production with a smooth quark matter to hadronic matter transition in relativistic heavy ion collisions, we study deuteron and triton productions from the coalescence of nucleons at the kinetic freezeout of these collisions. For central Au+Au collisions at center-of-mass energies $\sqrt{s_{\rm NN}}$ from 7.7 GeV to 200 GeV available at the Relativistic Heavy Ion Collider (RHIC), we find that the yield ratio $N_{\rm t}N_{\rm p}/N_{\rm d}^2$ of proton, deuteron, and triton is a monotonic function of collision energy. Our study confirms the results from similar studies based on different dynamic model, which have either no phase transition or a crossover transition between the quark-gluon plasma and the hadronic matter, that this yield ratio does not show any nonmonotonic behavior in its collision-energy dependence.

DOI: 10.1103/PhysRevC.103.064909

I. INTRODUCTION

Light nuclei, such as deuteron (d), helium-3 (^{3}He), triton (^{3}H or t), helium-4 (^{4}He), hypertriton ($^3_\Lambda$H), and their antiparticles, have been observed in high energy nucleus-nucleus (AA), proton-nucleus (pA), and pp collisions at RHIC and the LHC [1–6]. Because of their potential role in the search for the critical point [7–9] of strongly interacting matter in heavy ion collisions [10–13], studying these loosely bound nuclei with binding energies much smaller than the temperature of the hot dense matter created in these collisions has recently received an increased attention [14–31]. Also, these studies are useful for understanding the production of light (anti)nuclei in cosmic rays and in dark matter experiments [32–35]. As to the use of light nuclei production to probe the QCD phase diagram in relativistic heavy ion collisions, it is mainly due to their composite structures that make their production mostly from nucleons close in phase space and thus sensitive to nucleon correlations and density fluctuations [10–13]. In particular, it has been suggested in Refs. [10,11,36] that the yield ratio $N_{\rm t}N_{\rm p}/N_{\rm d}^2$ of proton, deuteron, and triton in relativistic heavy ion collisions could show a nonmonotonic dependence on the collision energy as a result of the enhanced density fluctuations due to the spinodal instability during a first-order quark to hadronic matter phase transition and/or the long-range correlation if the produced matter is close to the critical point of the QCD matter.

The production of light nuclei in relativistic heavy ion collisions has been studied in various models, including the statistical hadronization model [37,38], the nucleon coalescence model [39,40], and dynamical models based on the kinetic theory [41]. In the statistical hadronization model, the yields of light nuclei are determined at the same chemical freezeout temperature and baryon chemical potential as those for identified hadrons like protons, pions, and kaons, while their spectra are calculated from a blast-wave model at the hadronic kinetic freezeout when hadrons undergo their last collisions. This model has successfully described light nuclei production in Pb+Pb collisions at $\sqrt{s_{NN}} = 2.76$ TeV at LHC [16].

In the coalescence model, light nuclei are formed at kinetic freezeout of heavy ion collisions from nucleons that are close in phase space. There have been various ways of implementing the coalescence model in the literature, and these include the naive coalescence model based on the introduction of a phenomenological coalescence radius in phase space [39,40], the phase-space coalescence model that takes into account the internal wave functions of light nuclei [42–45], and the coalescence model that further uses the phase-space information of nucleons from microscopic transport models [19,46–49].

In dynamic models for light nuclei production, these nuclei are treated as explicit degrees of freedom, and their production and destruction during the hadronic evolution stage in heavy ion collisions are described by appropriate hadronic reactions with cross sections that satisfy the detailed balance relations [50–52]. In particular, the studies in Refs. [51,52] have shown that the deuteron yield remains almost unchanged from the chemical freezeout to the kinetic freezeout as a result of the large deuteron production and destruction cross sections that keep the deuteron abundance in thermal

[*]kjsun@tamu.edu
[†]ko@comp.tamu.edu
[‡]linz@ecu.edu

and chemical equilibrium in the expanding hadronic matter with decreasing temperature but increasing baryon chemical potential.

All above models have been used in understanding the recent data from the STAR Collaboration on deuteron and triton in Au+Au collisions at $\sqrt{s_{\rm NN}}$= 7.7–200 GeV [53–55]. For the thermal model, it gives a good description of the deuteron yield but overestimates the triton yield. None of these models can, however, reproduce the nonmonotonic behavior or peak structure in the collision-energy dependence of the yield ratio $N_{\rm p}N_{\rm t}/N_{\rm d}^2$.

In the present paper, we investigate the production of deuteron and triton in most central Au+Au collisions at $\sqrt{s_{\rm NN}}$ = 7.7-200 GeV by using the phase-space coalescence model based on kinetically freezeout nucleons from an improved multiphase transport (AMPT) model [56,57]. The AMPT model, which has been extensively used for studying various observables in heavy ion collisions at relativistic energies, includes the initial conditions from the HIJING model [58,59], the parton cascade via the ZPC model [60], and the hadronic transport based on the ART model [61] as well as a spatial quark coalescence model that converts kinetically freezeout quarks and antiquarks to the initial hadrons, resulting in a crossover phase transition. We find that the collision-energy dependence of the yield ratio $N_{\rm t}N_{\rm p}/N_{\rm d}^2$ from this model is essentially a constant. Our result is thus consistent with that obtained from a pure hadronic transport model [47] and also that from a hybrid model of hydrodynamics and hadronic transport with a crossover transition [62].

This paper is organized as follows. In Sec. II, we give a brief description of the nucleon phase-space coalescence model. We then present in Sec. III the energy dependence of the yield ratios $N_{\rm d}/N_{\rm p}$, $N_{\rm t}/N_{\rm p}$, and $N_{\rm t}N_{\rm p}/N_{\rm d}^2$ obtained from the coalescence model based on nucleons from the AMPT model. Finally, a conclusion is given in Sec. V.

II. THE NUCLEON COALESCENCE MODEL

For deuteron production from an emission source of protons and neutrons, its number in the coalescence model is calculated from the overlap of the proton and neutron phase-space distribution functions $f_{p,n}(\mathbf{x},\mathbf{p})$ with the Wigner function $W_{\rm d}(\mathbf{x},\mathbf{p})$ of the deuteron internal wave function [65], i.e.,

$$N_{\rm d} = g_{\rm d}\int d^3\mathbf{x}_1 d^3\mathbf{p}_1 d^3\mathbf{x}_2 d^3\mathbf{p}_2 f_n(\mathbf{x}_1,\mathbf{p}_1) \times f_p(\mathbf{x}_2,\mathbf{p}_2) W_{\rm d}(\mathbf{x},\mathbf{p}), \tag{1}$$

with $g_d = 3/4$ being the statistical factor for forming a deuteron of spin 1 from two spin 1/2 proton and neutron. Using the Gaussian or harmonic oscillator wave function for the internal wave function of a deuteron, as usually assumed in the coalescence model for deuteron production, its Wigner function is

$$W_{\rm d}(\mathbf{x},\mathbf{p}) = 8\exp\left(-\frac{x^2}{\sigma_d^2} - \sigma_d^2 p^2\right) \tag{2}$$

and is normalized according to $\int d^3\mathbf{x}\int d^3\mathbf{p}\, W_d(\mathbf{x},\mathbf{p}) = (2\pi)^3$. In the above, $\mathbf{x}$ and $\mathbf{p}$ are, respectively, the relative coordinate and momentum of the two nucleons in a deuteron, defined together with their center-of-mass coordinate $\mathbf{X}$ and momentum $\mathbf{P}$ by [45,66,67]

$$\mathbf{X} = \frac{\mathbf{x}_1+\mathbf{x}_2}{2}, \quad \mathbf{x} = \frac{\mathbf{x}_1-\mathbf{x}_2}{\sqrt{2}},$$
$$\mathbf{P} = \mathbf{p}_1+\mathbf{p}_2, \quad \mathbf{p} = \frac{\mathbf{p}_1-\mathbf{p}_2}{\sqrt{2}}. \tag{3}$$

The parameter σ in Eq. (2) is related the root-mean-square radius $r_{\rm d}$ of deuteron by $\sigma_d = \sqrt{4/3}\, r_{\rm d} \approx 2.26$ fm and is much smaller than the size of the hadronic system considered in the present study. We note that using the more realistic Hulthén wave function [68] for the deuteron, which can be represented by 15 Guassian functions with different size parameters [66], gives essentially the same deuteron yield in central Au+Au collisions.

Similarly, the number of tritons from the coalescence of two neutrons and one proton is given by

$$N_{\rm t} = g_t \int d^3\mathbf{x}_1 d^3\mathbf{p}_1 d^3\mathbf{x}_2 d^3\mathbf{p}_2 d^3\mathbf{x}_3 d^3\mathbf{p}_3 f_n(\mathbf{x}_1,\mathbf{p}_1) \times f_n(\mathbf{x}_2,\mathbf{p}_2) f_p(\mathbf{x}_3,\mathbf{p}_3) W_{\rm t}(\mathbf{x},\boldsymbol{\lambda},\mathbf{p},\mathbf{p}_\lambda), \tag{4}$$

where $g_t = 1/4$ is the statistical factor for the formation of a spin 1/2 triton from two spin 1/2 neutrons and one spin 1/2 proton. As for deuteron, we take the triton Wigner function to also have a Gaussian form,

$$W_{\rm t}(\mathbf{x},\boldsymbol{\lambda},\mathbf{p},\mathbf{p}_\lambda) = 8^2\exp\left(-\frac{x^2}{\sigma_{\rm t}^2} - \frac{\lambda^2}{\sigma_{\rm t}^2} - \sigma_{\rm t}^2 p^2 - \sigma_{\rm t}^2 p_\lambda^2\right), \tag{5}$$

where $\mathbf{x}$ and $\mathbf{p}$ are defined as in Eq. (3), and $\boldsymbol{\lambda}$ and $\mathbf{p}_\lambda$ are the additional relative coordinate and momentum. The latter are defined together with the center-of-mass coordinate $\mathbf{X}$ and momentum $\mathbf{P}$ of the nucleons in triton by [45,66,67]

$$\mathbf{X} = \frac{\mathbf{x}_1+\mathbf{x}_2+\mathbf{x}_3}{3}, \quad \boldsymbol{\lambda} = \frac{\mathbf{x}_1+\mathbf{x}_2-2\mathbf{x}_3}{\sqrt{6}},$$
$$\mathbf{P} = \mathbf{p}_1+\mathbf{p}_2+\mathbf{p}_3, \quad \mathbf{p}_\lambda = \frac{\mathbf{p}_1+\mathbf{p}_2-2\mathbf{p}_3}{\sqrt{6}}. \tag{6}$$

The parameter $\sigma_{\rm t}$ in Eq. (5) is related to the root-mean-square radius $r_{\rm t}$ of triton by $\sigma_{\rm t} = r_{\rm t} = 1.59$ fm [69]. We note that the coordinate transformations in Eqs. (3) and (6) conserve the phase-space volume, although not separately the volumes in coordinate and momentum spaces.

III. LIGHT NUCLEI PRODUCTION FROM THE AMPT MODEL

In the present work, we use the improved AMPT model of Ref. [57], which gives a better description of baryon production in relativistic heavy ion collisions than the usual AMPT model, to provide the phase-space information of nucleons needed for the production of deuteron and triton via the coalescence model. Specifically, from the kinetically freezeout nucleons given by AMPT with each one having a freezeout

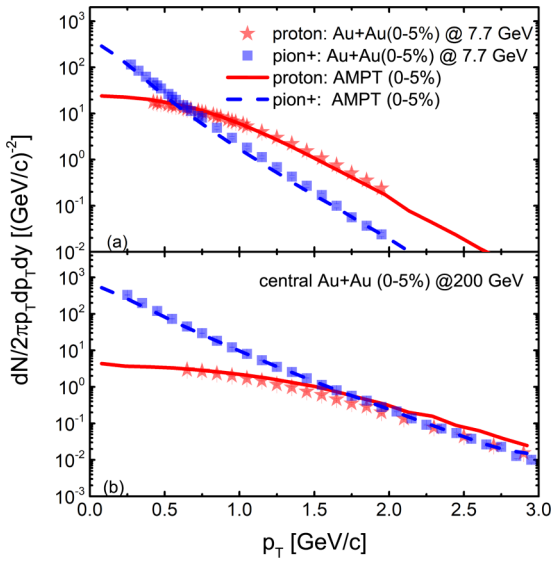

FIG. 1. Transverse momentum (p_T) spectra of protons and pions in 0–5% central Au+Au collisions at $\sqrt{s_{NN}} = 7.7$ GeV [panel (a)] and 200 GeV [panel (b)]. Theoretical results are shown by solid lines for protons and dashed lines for pions, while the experimental data from Refs. [63,64] for protons and pions are denoted by solid stars and squares, respectively. Data for protons at $\sqrt{s_{NN}} = 200$ GeV are corrected for the weak-decay contribution from hyperons.

position, momentum, and time, the probability for a proton and a neutron to form a deuteron is calculated from Eq. (1) by using their relative coordinate and momentum obtained after free streaming the nucleon with an earlier freezeout time to the later freezeout time of the other nucleon. A similar procedure is used in calculating the probability from Eq. (4) for two neutrons and one proton to coalesce into a triton, i.e., by free streaming the two nucleons of earlier freezeout times to the last freezeout time of the remaining nucleon.

We first show in Fig. 1 the transverse momentum (p_T) spectra of protons (solid lines) and pions (dashed lines) in 0–5% central Au+Au collisions at $\sqrt{s_{NN}} = 7.7$ GeV [panel (a)] and 200 GeV [panel (b)] obtained from the theoretical calculations. They are seen to describe fairly well the experimental data from Refs. [63,64,70], shown by solid stars and squares for protons and pions, respectively, confirming the success of the improved AMPT model of Ref. [57] in describing proton production in relativistic heavy ion collisions at RHIC energies.

We then show in the left window of Fig. 2 the yield ratio N_d/N_p (d/p) of deuteron to proton and N_t/N_p (t/p) of triton to proton as functions of the collision energy $\sqrt{s_{NN}}$. Results from the AMPT model, denoted by lines with solid squares, are seen to overestimate the measured d/p ratio (solid stars) by about a factor of three and t/p ratio (open stars) by about a factor of nine for all collision energies from 7.7 GeV to 200 GeV. The overestimation of deuteron production has also been noticed in Ref. [46] based on an earlier version of the AMPT model. This is due to the smaller hadronization hypersurface in the AMPT model compared to that from the hydrodynamic model [72], which has been shown to describe very well the deuteron and triton yields measured in experiments [62], after including the hadronic after burner and then using the nucleon coalescence model to describe the production of light nuclei. As a result, nucleons from the AMPT model occupy a smaller volume at kinetic freezeout and thus have larger probabilities to coalesce into deuterons and tritons than those from the hydrodynamic model. Improved treatments of partonic evolution and hadronization in AMPT are thus needed but are beyond the scope of the present study.

The right window of Fig. 2 shows the yield ratio $N_t N_p/N_d^2$ in central Au+Au collisions as a function of the collision energy $\sqrt{s_{NN}}$. It is seen that except for $\sqrt{s_{NN}} < 20$ GeV, where the central value of this ratio slightly increases with decreasing collision energy, it has almost a constant value of around 0.4, which is slightly larger than the value of around

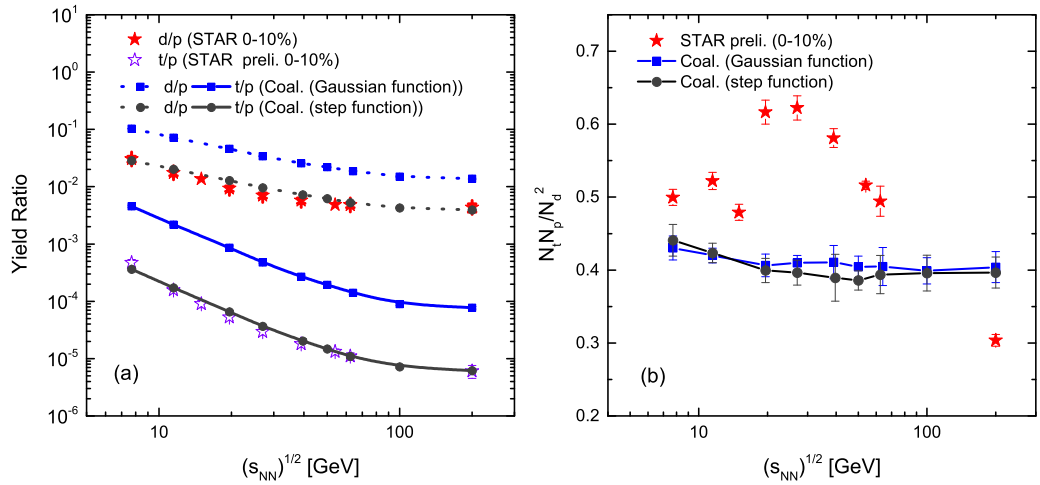

FIG. 2. The yield ratio N_d/N_p of deuteron to proton and N_t/N_p of triton to proton (left window) as well as the yield ratio $N_t N_p/N_d^2$ (right window) as functions of the collision energy $\sqrt{s_{NN}}$ in central Au+Au collisions. Results from the AMPT model are denoted by lines with filled squares and circles obtained by using Gaussian and step functions, respectively. The experimental data taken from Refs. [47,53–55] are shown by solid and open stars after correcting the weak-decay contribution from hyperons to protons [71].

0.29 obtained by assuming a uniform distribution of nucleons in the analytical calculations of Refs. [10,11]. The monotonic behavior of the yield ratio $N_t N_p/N_d^2$ obtained in the present study contradicts the nonmonotonic behavior seen in the data, shown by solid stars in the right window of Fig. 2. This result supports the suggestion in Refs. [10–13] that a nonmonotonic dependence of this ratio on the energy of heavy ion collisions could be due to a first-order phase transition in the produced matter or the approach to the critical point of the QCD matter.

Our result on the $N_t N_p/N_d^2$ ratio is similar to that in a recent study [62] obtained from the nucleon coalescence model by using kinetic freezeout nucleons from a new three-dimensional hybrid dynamical model (IEBE-MUSIC) with a smooth crossover equation of state without a QCD critical point, where the predicted value of the yield ratio $N_t N_p/N_d^2$ is also almost a constant as a function of collision energy. A similar conclusion of a collision energy independent $N_t N_p/N_d^2$ ratio has also been obtained in Ref. [47] based on the coalescence of kinetically freezeout nucleons from a pure hadronic JAM transport model by using step Wigner functions for the deuteron and triton. To see the effects of using different Wigner functions for the deuteron and triton in the coalescence model, we repeat our study with the Heaviside step functions:

$$W_d = \theta(\Delta r_d - |\mathbf{x}|)\theta(\Delta p_d - |\mathbf{p}|), \tag{7}$$

$$W_t = \theta(\Delta r_t - |\mathbf{x}|)\theta(\Delta r_t - |\boldsymbol{\lambda}|)\theta(\Delta p_t - |\mathbf{p}|)\theta(\Delta p_t - |\mathbf{p}_\lambda|), \tag{8}$$

where $\Delta r_{d,t}$ and $\Delta p_{d,t}$ are parameters. As usually done in coalescence model with step Wigner functions [47,49,73], we fix the values of Δr_d and Δr_t by requiring them to give the same root mean square radii of deuteron and triton as the empirical ones. This leads to $\Delta r_d = \sqrt{10/3} r_d = 3.6$ fm and $\Delta r_t = \sqrt{5/2} r_t = 2.5$ fm. We then determine the values for Δp_d and Δp_t by fitting the experimental deuteron and triton yields. We find that a single set of parameters $\Delta p_d = 86.8$ MeV and $\Delta p_t = 118$ MeV can well describe the d/p and t/p ratios from $\sqrt{s_{NN}} = 7.7$ GeV to 200 GeV as shown by the solid lines with filled circles in the left widow of Fig. 2. The collision-energy dependence of the yield ratio $N_t N_p/N_d^2$ from using the step Wigner functions is shown by the solid line with filled circles in the right window of Fig. 2 and is seen to have a similar behavior as that from using the Gaussian Wigner functions. The fact that the yield ratio $N_t N_p/N_d^2$ is insensitive to the details of the coalescence model indicates that its monotonic dependence on the collision energy is mainly due to the absence of nucleon density fluctuations in these collisions. Results from our study as well as those from Refs. [47,62] thus indicates that in dynamic models for relativistic heavy ion collisions without the QGP to hadronic matter phase transition or with a crossover transition, the yield ratio $N_t N_p/N_d^2$ would not show any nonmonotonic dependence on the collision energy. This result is useful for the beam energy scan (BES) program at RHIC to search for the QCD critical point in heavy ion collisions.

IV. CONCLUSIONS

In the present paper, we have studied light nuclei production from central Au+Au collision at $\sqrt{s_{NN}} = 7.7 - 200$ GeV in the nucleon coalescence model based on the phase-space distribution of kinetically freezeout nucleons from an improved AMPT model. We have found that the yield ratio $N_t N_p/N_d^2$ varies monotonically as a function of collision energy. Our results from the AMPT model, which only has a smooth crossover from the partonic matter to the hadronic matter, confirm those from other dynamic models that have either no phase transition or only a crossover transition. A deviation of experimentally measured collision-energy dependence of this ratio from these results, especially a nonmonotonic behavior, could hint at the occurrence of a non-smooth phase transition in the produced matter for collisions at certain energies. Since light nuclei production from the coalescence of nucleons depends on the size of homogeneity in the nucleon emission source, a simultaneous study of their production and the Hanbury-Brown-Twiss (HBT) radii as a function of the collision energy within the same dynamic model will be very useful for the determination of the location of the critical point in the QCD phase diagram from heavy ion collision in the BES program at RHIC as well as at future FAIR in GSI and NICA in Dubna.

ACKNOWLEDGMENTS

The authors thank Xiaofeng Luo, Hui Liu, Wenbin Zhao, and Shanshan Cao for helpful discussions. This work was supported in part by the US Department of Energy under Award No. DE-SC0015266, the Welch Foundation under Grant No. A-1358, and National Science Foundation under Grant No. 2012947.

[1] B. I. Abelev *et al.* (STAR Collaboration), Science **328**, 58 (2010).
[2] H. Agakishiev *et al.* (STAR Collaboration), Nature (London) **473**, 353 (2011) [Erratum: Nature (London) **475**, 412 (2011)].
[3] N. Sharma *et al.* (ALICE Collaboration), J. Phys. G **38**, 124189 (2011).
[4] J. Adam *et al.* (STAR Collaboration), Nat. Phys. **16**, 409 (2020).
[5] S. Acharya *et al.* (ALICE Collaboration), Phys. Rev. C **101**, 044906 (2020).
[6] S. Acharya *et al.* (ALICE Collaboration), Eur. Phys. J. C 80 (2020) 889.
[7] A. Bzdak, S. Esumi, V. Koch, J. Liao, M. Stephanov, and N. Xu, Phys. Rep. **853**, 1 (2020).
[8] X. Luo, S. Shi, N. Xu, and Y. Zhang, Particles **3**, 278 (2020).
[9] D. Oliinychenko, in 28th International Conference on Ultra-relativistic Nucleus-Nucleus Collisions (Quark Matter 2019) Wuhan, China, November 4–9, 2019 (2020), arXiv:2003.05476.

[10] K.-J. Sun, L.-W. Chen, C. M. Ko, and Z. Xu, Phys. Lett. B **774**, 103 (2017).
[11] K.-J. Sun, L.-W. Chen, C. M. Ko, J. Pu, and Z. Xu, Phys. Lett. B **781**, 499 (2018).
[12] E. Shuryak and J. M. Torres-Rincon, Phys. Rev. C **100**, 024903 (2019).
[13] E. Shuryak and J. M. Torres-Rincon, Phys. Rev. C **101**, 034914 (2020).
[14] Y.-G. Ma, J.-H. Chen, and L. Xue, Front. Phys. (Beijing) **7**, 637 (2012).
[15] A. Andronic, P. Braun-Munzinger, K. Redlich, and J. Stachel, Nature (London) **561**, 321 (2018).
[16] P. Braun-Munzinger and B. Dönigus, Nucl. Phys. A **987**, 144 (2019).
[17] J. Chen, D. Keane, Y.-G. Ma, A. Tang, and Z. Xu, Phys. Rept. **760**, 1 (2018).
[18] S. Bazak and S. Mrowczynski, Mod. Phys. Lett. A **33**, 1850142 (2018).
[19] Z.-J. Dong, G. Chen, Q.-Y. Wang, Z.-L. She, Y.-L. Yan, F.-X. Liu, D.-M. Zhou, and B.-H. Sa, Eur. Phys. J. A **54**, 144 (2018).
[20] F. Bellini and A. P. Kalweit, Phys. Rev. C **99**, 054905 (2019).
[21] K.-J. Sun, C. M. Ko, and B. Dönigus, Phys. Lett. B **792**, 132 (2019).
[22] X. Xu and R. Rapp, Eur. Phys. J. A **55**, 68 (2019).
[23] Y. Cai, T. D. Cohen, B. A. Gelman, and Y. Yamauchi, Phys. Rev. C **100**, 024911 (2019).
[24] S. Mrowczynski and P. Slon, Acta Phys. Pol. B **51**, 1739 (2020).
[25] M. Kachelriess, S. Ostapchenko, and J. Tjemsland, Eur. Phys. J. A **56**, 4 (2020).
[26] S. Mrowczynski, Eur. Phys. J. Special Topics **229**, 3559 (2020).
[27] B. Dönigus, Int. J. Mod. Phys. E **29**, 2040001 (2020).
[28] T. Shao, J. Chen, C. M. Ko, K.-J. Sun, and Z. Xu, Chinese Phys. C **44**, 114001 (2020).
[29] V. Vovchenko, B. Dönigus, B. Kardan, M. Lorenz, and H. Stoecker, Phys. Lett. B **809**, 135746 (2020).
[30] Y. Ye, Y. Wang, Q. Li, D. Lu, and F. Wang, Phys. Rev. C **101**, 034915 (2020).
[31] S. Bazak and S. Mrowczynski, Eur. Phys. J. A **56**, 193 (2020).
[32] V. Vagelli (AMS Collaboration), Nuovo Cim. C **42**, 173 (2019).
[33] A. Kounine and S. Ting (AMS Collaboration), PoS ICHEP **340**, 732 (2019).
[34] K. Blum, Kenny Chun Yu Ng, R. Sato, and M. Takimoto, Phys. Rev. D **96**, 103021 (2017).
[35] V. Poulin, P. Salati, I. Cholis, M. Kamionkowski, and J. Silk, Phys. Rev. D **99**, 023016 (2019).
[36] K.-J. Sun, F. Li, and C. M. Ko, Phys. Lett. B **816**, 136258 (2021).
[37] J. Cleymans and H. Satz, Z. Phys. C **57**, 135 (1993).
[38] P. Braun-Munzinger, V. Koch, T. Schäfer, and J. Stachel, Phys. Rept. **621**, 76 (2016).
[39] H. Gutbrod, A. Sandoval, P. Johansen, A. M. Poskanzer, J. Gosset, W. Meyer, G. Westfall, and R. Stock, Phys. Rev. Lett. **37**, 667 (1976).
[40] L. Csernai and J. I. Kapusta, Phys. Rept. **131**, 223 (1986).
[41] P. Danielewicz and G. Bertsch, Nucl. Phys. A **533**, 712 (1991).
[42] H. Sato and K. Yazaki, Phys. Lett. B **98**, 153 (1981).
[43] R. Scheibl and U. W. Heinz, Phys. Rev. C **59**, 1585 (1999).
[44] S. Mrowczynski, Acta Phys. Polon. B **48**, 707 (2017).
[45] K.-J. Sun and L.-W. Chen, Phys. Rev. C **95**, 044905 (2017).
[46] L. Zhu, C. M. Ko, and X. Yin, Phys. Rev. C **92**, 064911 (2015).
[47] H. Liu, D. Zhang, S. He, K.-j. Sun, N. Yu, and X. Luo, Phys. Lett. B **805**, 135452 (2020).
[48] Y. B. Ivanov and A. Soldatov, Eur. Phys. J. A **53**, 218 (2017).
[49] S. Sombun, K. Tomuang, A. Limphirat, P. Hillmann, C. Herold, J. Steinheimer, Y. Yan, and M. Bleicher, Phys. Rev. C **99**, 014901 (2019).
[50] Y. Oh, Z.-W. Lin, and C. M. Ko, Phys. Rev. C **80**, 064902 (2009).
[51] S. Cho, T. Song, and S. H. Lee, Phys. Rev. C **97**, 024911 (2018).
[52] D. Oliinychenko, L.-G. Pang, H. Elfner, and V. Koch, Phys. Rev. C **99**, 044907 (2019).
[53] J. Adam *et al.* (STAR Collaboration), Phys. Rev. C **99**, 064905 (2019).
[54] D. Zhang (for STAR Collaboration), JPS Conf. Proc. **32**, 010069 (2020).
[55] D. Zhang (for STAR Collaboration), Nucl. Phys. A **1005**, 121825 (2020).
[56] Z.-W. Lin, C. M. Ko, B.-A. Li, B. Zhang, and S. Pal, Phys. Rev. C **72**, 064901 (2005).
[57] Y. He and Z.-W. Lin, Phys. Rev. C **96**, 014910 (2017).
[58] M. Gyulassy and X.-N. Wang, Comput. Phys. Commun. **83**, 307 (1994).
[59] X.-N. Wang and M. Gyulassy, Phys. Rev. D **44**, 3501 (1991).
[60] B. Zhang, Comput. Phys. Commun. **109**, 193 (1998).
[61] B.-A. Li and C. M. Ko, Phys. Rev. C **52**, 2037 (1995).
[62] W. Zhao, C. Shen, C. M. Ko, Q. Liu, and H. Song, Phys. Rev. C **102**, 044912 (2020).
[63] L. Adamczyk *et al.* (STAR Collaboration), Phys. Rev. C **96**, 044904 (2017).
[64] S. S. Adler *et al.* (PHENIX Collaboration), Phys. Rev. C **69**, 034909 (2004).
[65] M. Gyulassy, K. Frankel, and E. A. Remler, Nucl. Phys. A **402**, 596 (1983).
[66] L.-W. Chen, C. Ko, and B.-A. Li, Nucl. Phys. A **729**, 809 (2003).
[67] K.-J. Sun and L.-W. Chen, Phys. Lett. B **751**, 272 (2015).
[68] P. E. Hodgson, *Nuclear Reactions and Nuclear Structure* (Clarendon, Oxford, 1971), p. 453.
[69] G. Ropke, Phys. Rev. C **79**, 014002 (2009).
[70] B. Abelev *et al.* (ALICE Collaboration), Phys. Rev. C **88**, 044910 (2013).
[71] L. Adamczyk *et al.* (STAR Collaboration), Phys. Rev. Lett. **121**, 032301 (2018).
[72] B. Fu, K. Xu, X.-G. Huang, and H. Song, Phys. Rev. C **103**, 024903 (2021).
[73] Q. Li, Y. Wang, X. Wang, and C. Shen, Sci. China Phys. Mech. Astron. **59**, 622001 (2016).